scientific reports

OPEN

PolyQ-expanded proteins impair cellular proteostasis of ataxin-3 through sequestering the co-chaperone HSJ1 into aggregates

Hong-Wei Yue[1,2], Jun-Ye Hong[1,2], Shu-Xian Zhang[1,2], Lei-Lei Jiang[1] & Hong-Yu Hu[1✉]

Polyglutamine (polyQ) expansion of proteins can trigger protein misfolding and amyloid-like aggregation, which thus lead to severe cytotoxicities and even the respective neurodegenerative diseases. However, why polyQ aggregation is toxic to cells is not fully elucidated. Here, we took the fragments of polyQ-expanded (PQE) ataxin-7 (Atx7) and huntingtin (Htt) as models to investigate the effect of polyQ aggregates on the cellular proteostasis of endogenous ataxin-3 (Atx3), a protein that frequently appears in diverse inclusion bodies. We found that PQE Atx7 and Htt impair the cellular proteostasis of Atx3 by reducing its soluble as well as total Atx3 level but enhancing formation of the aggregates. Expression of these polyQ proteins promotes proteasomal degradation of endogenous Atx3 and accumulation of its aggregated form. Then we verified that the co-chaperone HSJ1 is an essential factor that orchestrates the balance of cellular proteostasis of Atx3; and further discovered that the polyQ proteins can sequester HSJ1 into aggregates or inclusions in a UIM domain-dependent manner. Thereby, the impairment of Atx3 proteostasis may be attributed to the sequestration and functional loss of cellular HSJ1. This study deciphers a potential mechanism underlying how PQE protein triggers proteinopathies, and also provides additional evidence in supporting the hijacking hypothesis that sequestration of cellular interacting partners by protein aggregates leads to cytotoxicity or neurodegeneration.

Abbreviations

Atx3	Ataxin-3
Atx7	Ataxin-7
CFTR	Cystic fibrosis transmembrane regulator
CREB	CAMP-response element binding protein
HSJ1	*Homo sapiens* J-domain protein
HSP40	Heat shock protein 40
Htt	Huntingtin
JD	J domain
NLS	Nuclear localization signal
polyQ	Polyglutamine
PQE	PolyQ expansion or polyQ-expanded
PQC	Protein quality control
RIPA	Radio-immune precipitation assay
RT-PCR	Reverse transcription-polymerase chain reaction
SCA3	Spinal cerebellar ataxia
SOD1	Copper-zinc superoxide dismutase 1
Ub	Ubiquitin

[1]State Key Laboratory of Molecular Biology, Shanghai Institute of Biochemistry and Cell Biology, Center for Excellence in Molecular Cell Science, Chinese Academy of Sciences, Shanghai 200031, People's Republic of China. [2]University of Chinese Academy of Sciences, Beijing 100049, People's Republic of China. ✉email: hyhu@sibcb.ac.cn

UIM   Ubiquitin-interacting motif
WT   Wild type

Polyglutamine (polyQ) diseases are one group of neurodegenerative disorders typically characterized by the aberrant expansion of *CAG* repeats that encodes a polyQ tract in the pathogenic protein[1,2]. The existing polyQ tract that extends over a certain threshold will become an amyloid core and thus trigger protein misfolding and aggregation[3]. It is well-known that protein aggregation is a pathological hallmark shared among diverse neuro-degenerative diseases[4–8]. However, why amyloid-like aggregation of polyQ proteins is toxic to cells, especially to neurons, remains only partially understood. As each polyQ disease is caused by one definitive pathogenic protein that possesses a clear amyloidogenic core, the expanded polyQ tract, it becomes an excellent model for studying the patho-mechanism of protein aggregation-related diseases[9]. The pathogenic polyQ-expanded (PQE) proteins can be cleaved to generate small fragments by intracellular proteases[10]. So far, different N-terminal fragments of PQE huntingtin (Htt)[11–13] and ataxin-7 (Atx7)[14–16] and the C-terminal fragments of pathogenic ataxin-3 (Atx3)[17–20] have been identified and characterized. These small fragments with expanded polyQ tracts are sufficient to cause cytotoxicities or produce disease phenotypes. Therefore, the small fragments with polyQ tracts have been applied in many cellular research systems and animal models to elucidate the cytotoxicities and pathologies of polyQ diseases[21,22]. In our previous studies, we took several fragments of PQE Htt[23,24], Atx3[24,25] and Atx7[26] as models to address such a general question why polyQ aggregates are toxic to cells or neurons.

Recently, oligomers and aggregates generated during protein misfolding are recognized as two major toxic species[27]. The soluble oligomers and deposited aggregates seem to exhibit cytotoxicities through diverse mecha-nisms. Protein oligomers expose their hydrophobic amino-acid residues to form sticky surfaces that are reported to aberrantly interact with key cellular factors[28] or disrupt phosphorlipid bilayers[29,30]. Protein aggregates depos-ited in cells usually form inclusion bodies, the common structures that can be visualized in different neurode-generative diseases[31–33]. Accumulating evidence supports that protein aggregates or inclusions are toxic to cells by sequestering or hijacking critical cellular components, including chaperones and co-chaperones[7,34–36], ubiquitin (Ub)-related proteins[24,37,38], and other specifically interacting partners[25,26]. These sequestration effects may cause loss-of-function of the hijacked components and thus lead to their cellular dysfunction and cytotoxicity. For example, polyQ aggregates as reported can sequester the HSP40 chaperone Sis1p, interfere with the normal func-tion of hijacked Sis1p, and consequently result in impairment of the cellular proteostasis[39]. Thus, the diversity of composition in protein aggregates or inclusions may be at least partially explained by the sequestration effect[40]. Diverse proteins appeared in the polyQ inclusions are potentially related to the cytotoxicity and pathological progression of the polyQ diseases.

Ataxin-3 (Atx3) is one of the deubiquitinating enzymes reported to be involved in different protein inclusion bodies[41,42]. As a polyQ tract-containing protein, Atx3 may experience polyQ expansion that leads to protein aggregation and the spinal cerebellar ataxia (SCA3)[8,43]. It should be noted that wild-type (WT) Atx3 other than its pathogenic one has also been identified in the polyQ inclusions, suggesting that the WT Atx3 protein may be sequestered into the aggregates in cells[17,44]. Our previous study unraveled that the proteasomal degradation of endogenous Atx3 is orchestrated delicately by HSJ1 (DNAJB2), a co-chaperone of HSP70[45]. HSJ1 (mainly HSJ1a and HSJ1b isoforms) belongs to a member of the DNAJ family proteins that are defined by the J domain (JD), and regulates the function of HSP70 chaperones[46]. HSP70 and its co-chaperones cooperate closely with the protein degradation machineries in a concerted proteostasis network[47].

We hypothesized that the involvement of endogenous Atx3 in the polyQ inclusions could account for the cytotoxic effects of the pathogenic PQE proteins. To address this issue, we applied the N-terminal fragments of PQE Atx7 and Htt proteins to examine the effect of polyQ aggregates on the cellular proteostasis of Atx3. We found that these PQE proteins promote proteasomal degradation of endogenous Atx3 and enhance its forma-tion of aggregates. We also confirmed our previous finding that HSJ1 functions as a dual modulator of Atx3 in degradation and stability[45]. Besides, the impairment of cellular proteostasis of Atx3 may be attributed to the sequestration of HSJ1 and its functional loss by the PQE proteins. This study provides some clues to understand-ing of the mechanism underlying why PQE protein is toxic to cells.

Results

PQE Atx7 and Htt reduce the soluble fraction of endogenous Atx3 but increase its insoluble aggregates.

Atx3 is a polyQ tract-containing protein that may co-aggregate with other PQE proteins and form amyloid-like inclusions in cells[17,44]. To examine the possible co-aggregation effect of the polyQ proteins on the cellular Atx3 level, we firstly applied the N-terminal fragment of PQE Atx7 ($Atx7_{93Q}$-N172) and per-formed supernatant/pellet fractionation experiment in HEK 293T cells. As shown in the result, expression of $Atx7_{93Q}$-N172 caused a remarkable decline of soluble Atx3 in the supernatant fraction; whereas it increased the insoluble aggregates appeared in the pellet (Fig. 1A). We then verified this effect in an N-terminal fragment of PQE Htt (Htt_{100Q}-N90). It showed a similar effect with $Atx7_{93Q}$-N172 on the endogenous Atx3 levels both in solu-ble and insoluble fractions (Fig. 1B). Considering that both $Atx7_{93Q}$-N172 and Htt_{100Q}-N90 form cytoplasmic aggregates or inclusions, we further determined to clarify whether the nucleus-localized form of $Atx7_{93Q}$-N172 (NLS-$Atx7_{93Q}$-N172) similarly influence the cellular Atx3 levels. The nucleus-localized construct formed nuclear inclusions (see Fig. 2C); it could also reduce the soluble Atx3 level but increase its insoluble fraction (Fig. 1C). All these results demonstrate that the PQE proteins can reduce the soluble Atx3 level but enhance formation of the aggregates, regardless of their polyQ-protein types or cellular localization.

PQE Atx7 and Htt reduce the overall level of intracellular Atx3.

As a remarkable decline of the soluble Atx3 fraction was observed in the supernatant, we wondered whether this reduction was due to its con-
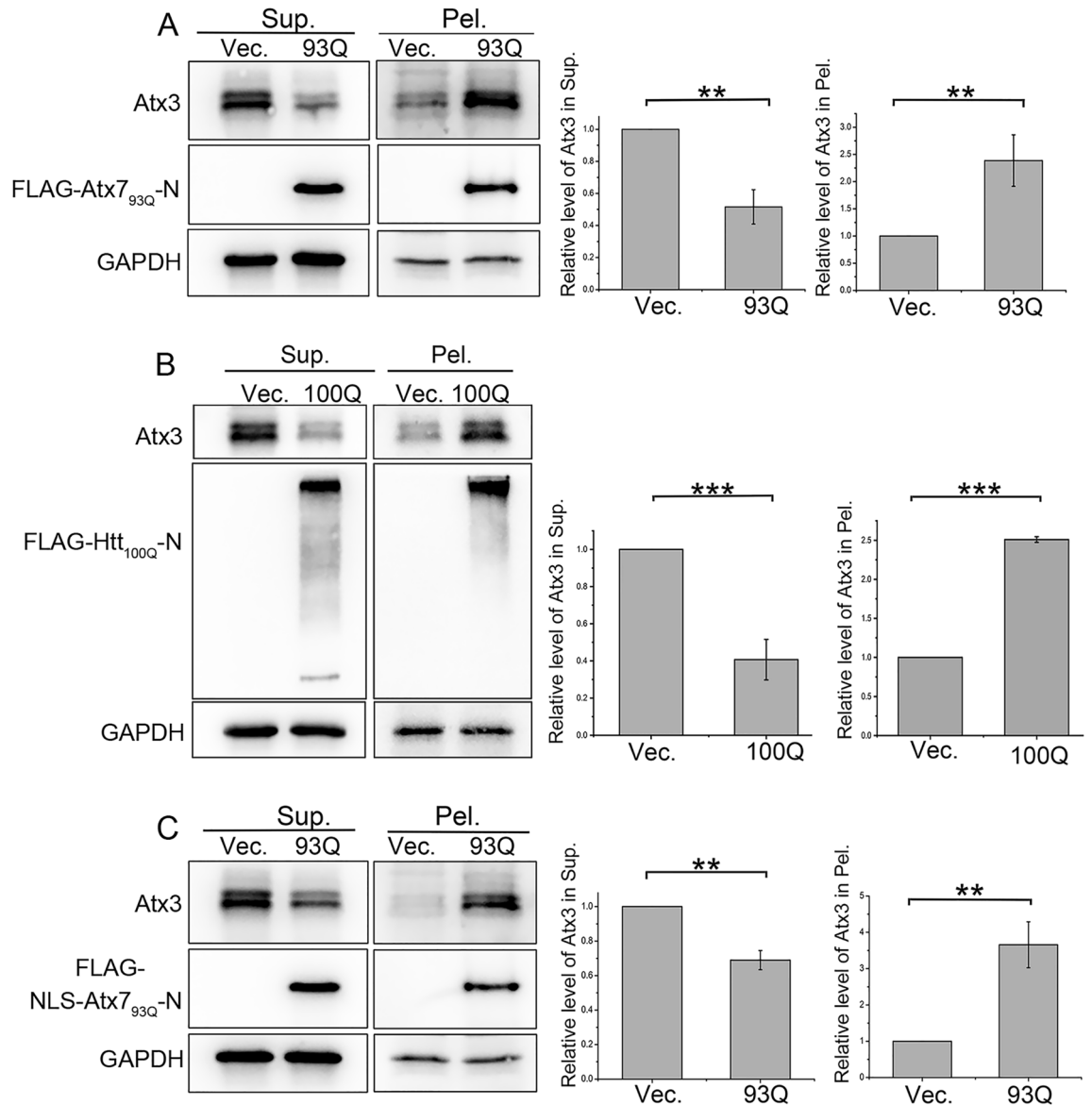
Figure 1. PQE Atx7 and Htt reduce the soluble fraction of intracellular Atx3 but increase the insoluble. (**A**) Effects of cytoplasm-localized Atx7$_{93Q}$-N172 on the supernatant and pellet fractions of Atx3. (**B**) As in (**A**), cytoplasm-localized Htt$_{100Q}$-N90. (**C**) As in (**A**), nucleus-localized NLS-Atx7$_{93Q}$-N172. HEK 293T cells were transfected with each indicated plasmid and the cell lysates were subjected to supernatant/pellet fractionation and Western blotting analysis. Indicated proteins were detected by using anti-FLAG, anti-Atx3 and anti-GAPDH antibodies. The two main bands indicate different isoforms of endogenous Atx3, Atx3-I and Atx3-II. Sup., supernatant; Pel., pellet. The gray values of Atx3 protein bands from three independent experiments were employed for statistical analysis. Data are shown as Means ± SEM (n = 3). **$p < 0.01$; ***$p < 0.001$.

version into insoluble fraction or reflected a decrease in the overall protein level. We thus extracted total intracellular protein of Atx3 by using the lysis buffer containing 8 M urea that may completely dissolve the aggregated form of Atx3, and then detected the overall protein level of endogenous Atx3 by Western blotting. The results showed that Atx7$_{93Q}$-N172, whether localized in cytoplasm or nucleus, caused a significant decrease in the total protein level of Atx3 (Fig. 2A). Similarly, Htt$_{100Q}$-N90 could also reduce the total Atx3 level (Fig. 2B). Besides, as visualized by confocal microscopy, the immunofluorescence intensity of endogenous Atx3 dropped down obviously upon formation of the Atx7$_{93Q}$-N172 inclusions (Fig. 2C). Consistently, we also observed a decrease of the Atx3 fluorescence in the cells with formation of the Htt$_{100Q}$-N90 inclusions (Fig. 2D). So, we proposed that the PQE proteins reduce the soluble protein of endogenous Atx3 and thus cause decrease of the overall protein level, albeit the insoluble Atx3 aggregates increase substantially.

To examine whether the decrease of Atx3 level was caused by mRNA variation, we performed quantitative RT-PCR assay for evaluating the mRNA level changes upon exogenous expression of PQE proteins. The qPCR data showed that the mRNA levels of Atx3 remained almost unchanged when the Atx7$_{93Q}$-N172 or Htt$_{100Q}$-N90 protein was exogenously over-expressed in cells (Supplemental Fig. 1), suggesting that overexpression of the
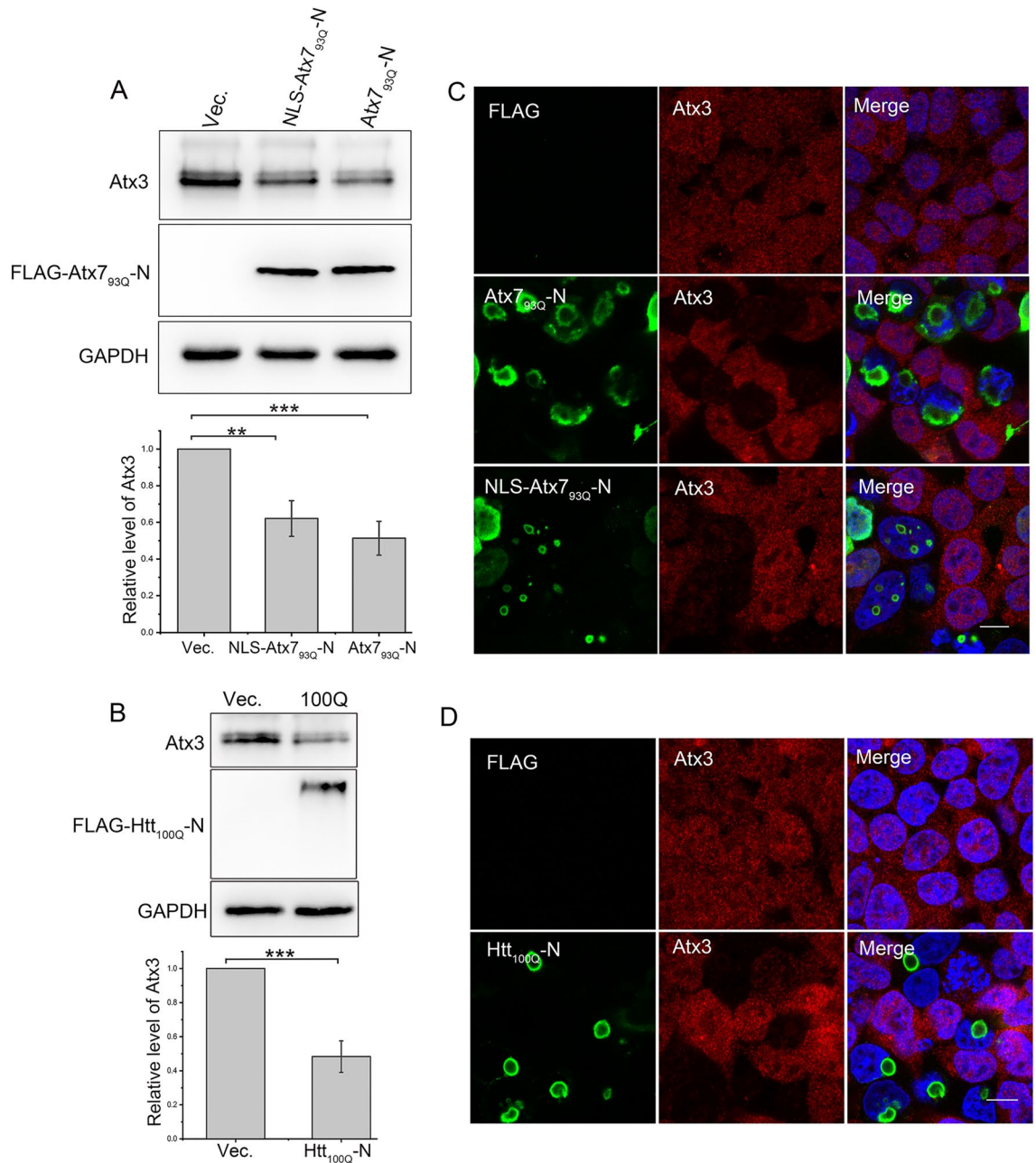
Figure 2. PQE Atx7 and Htt reduce the overall protein level of intracellular Atx3. (**A**) Effect of Atx7$_{93Q}$-N172 or NLS-Atx7$_{93Q}$-N172 on the overall level of Atx3. (**B**) Effect of Htt$_{100Q}$-N90 on the overall level of Atx3. HEK 293T cells were transfected with each indicated plasmid and the total-protein samples were prepared and subjected to Western blotting. Indicated proteins were detected by using anti-FLAG, anti-Atx3 and anti-GAPDH antibodies. Data are shown as Means ± SEM (n = 3). **$p < 0.01$; ***$p < 0.001$. (**C**) Immunofluorescence imaging showing that the cytoplasmic or nuclear Atx7$_{93Q}$-N172 inclusions cause fluorescence weakening of the endogenous Atx3. (**D**) As in (**C**), Htt$_{100Q}$-N90. HEK 293T cells were transfected with each indicated plasmid and then subjected to immunofluorescence staining and confocal microscopic imaging. PolyQ proteins were stained with anti-FLAG antibody (green), Atx3 was stained with anti-Atx3 antibody (red), and nuclei were stained with Hoechst (blue). Scale bar = 10 μm.

PQE proteins has little effect on the mRNA level of Atx3. This result excludes the possibility that the decrease of Atx3 level is due to its transcriptional alteration.

PQE Atx7 and Htt promote proteasomal degradation of intracellular Atx3. As well acknowledged, cellular proteostasis is finely regulated by an integrated network of chaperones and protein degradation system[48–51]. However, the misfolded proteins that escape surveillance of the degradation machineries would form insoluble aggregates deposited in cells[27]. Therefore, we speculate that, upon expression of the PQE proteins,
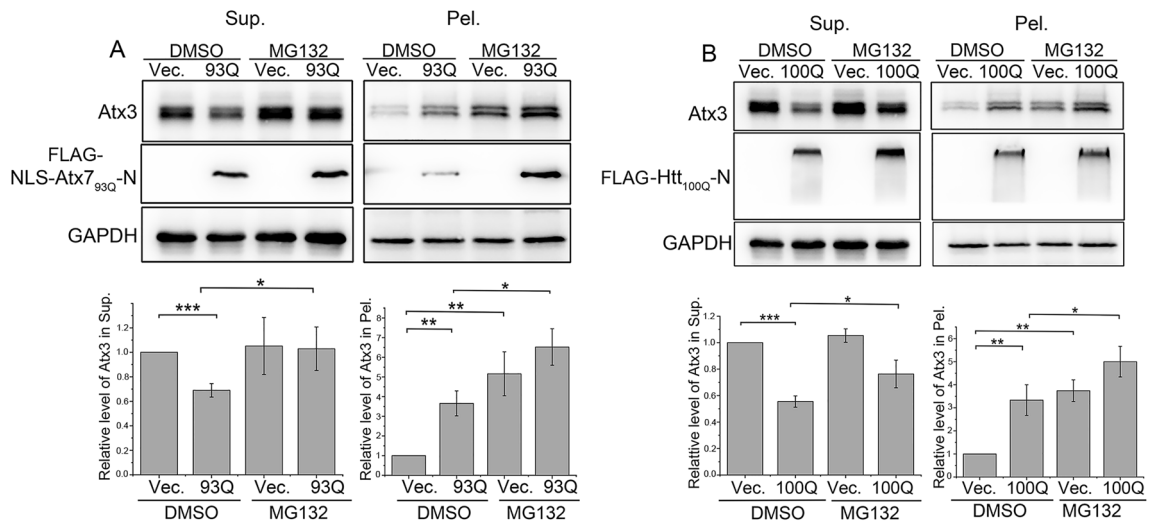
Figure 3. PQE Atx7 and Htt cause the reduction of soluble Atx3 through promoting proteasomal degradation. (**A**) Inhibition of proteasome suppresses the decline of soluble Atx3 caused by NLS-Atx7$_{93Q}$-N172. (B) As in (A), by Htt$_{100Q}$-N90. HEK 293T cells were transfected with each indicated plasmid and treated with MG132 (10 μM) for 12 h before harvest. DMSO was set as a control. The cell lysates were subjected to supernatant/pellet fractionation and Western blotting. Indicated proteins were detected by using anti-FLAG, anti-Atx3 and anti-GAPDH antibodies. Sup., supernatant; Pel., pellet. Data are shown as Means ± SEM (n = 3). *$p < 0.05$; **$p < 0.01$; ***$p < 0.001$.

the cellular proteostasis of Atx3 is somehow disrupted, resulting in an increase of protein aggregates and a massive decline of soluble Atx3 that may be attributed to protein degradation.

To verify the role of proteasomal degradation pathway in reduction of the Atx3 level triggered by the PQE proteins, we examined the effect of the proteasome inhibitor MG132 on the degradation of endogenous Atx3. The results showed that, NLS-Atx7$_{93Q}$-N172 and Htt$_{100Q}$-N90 both caused reduction of the soluble Atx3 level, while MG132 treatment, to some extent, could reverse the decrease of Atx3 in the supernatant fraction (Fig. 3A, B). As expected, MG132 treatment aggravated the increase of the aggregated form of Atx3 caused by the PQE proteins (Fig. 3A, B), which may be attributed to the inefficient degradation of Atx3 upon inhibition of proteasome. We then examined the possible role of autophagy pathway in Atx3 degradation by using chloroquine (CQ), a lysosomal degradation inhibitor. As a result, CQ treatment could up-regulate the LC3-II level remarkably (Supplemental Fig. 2A, C), indicating the effective inhibition of autophagic degradation. However, blocking of the autophagic degradation exhibited no significant influence on the decline of Atx3 caused by Atx7$_{93Q}$-N172 or Htt$_{100Q}$-N90 (Supplemental Fig. 2B, D). Similarly, we also observed the increase of the aggregated form of Atx3 in the pellet fraction upon inhibition of autophagy. As autophagy is widely recognized as an important pathway to scavenge protein aggregates[52,53], it may exert a role in the clearance of Atx3 aggregates in cells. So, we conclude that the PQE proteins reduce the soluble form of intracellular Atx3 mainly through promoting proteasomal degradation.

HSJ1a suppresses the degradation of intracellular Atx3 through its UIM domain. We previously revealed that HSJ1a promotes proteasomal degradation of Atx3 through interacting with HSP70 mainly by the function of the J domain, while its UIM domain binds to the Ub chains conjugated in Atx3 and maintains its protein level[45]. Thus, we examined the effect of HSJ1a on the degradation of endogenous Atx3 triggered by the PQE proteins. We co-expressed full-length HSJ1a (HSJ1a-FL) (Fig. 4A) with Atx7$_{93Q}$-N172 or NLS-Atx7$_{93Q}$-N172 in HEK 293T cells and performed supernatant/pellet fractionation. The results showed that overexpression of HSJ1a-FL could both alleviate the reduction of soluble Atx3 in supernatant and the increase of aggregated Atx3 in pellet (Fig. 4B and Supplemental Fig. 3A). This implied that HSJ1a has an important function in modulating the cellular proteostasis of Atx3. As known, the J domain of HSJ1a exhibits a co-chaperone activity for promoting Atx3 degradation and consequently attenuating its aggregation[45]. We thus over-expressed the JD-deleted construct (HSJ1a-ΔJD) with Atx7$_{93Q}$-N172 and found that, similar to HSJ1a-FL, HSJ1a-ΔJD was also able to reverse the reduction of soluble Atx3 caused by the PQE protein (Fig. 4C). Based on our previous finding that HSJ1a mainly suppresses the Atx3 degradation through its UIM domain[45], we over-expressed the UIM-domain mutant of HSJ1a (HSJ1a-UIM^{mut}) and revealed that the mutant failed to reverse the reduction of soluble Atx3 (Fig. 4D and Supplemental Fig. 3B). Together, these data reaffirm that HSJ1a suppresses the degradation of Atx3 through the UIM domain, and thus suggest that it is able to reverse the reduction of soluble Atx3 caused by the PQE proteins.

PQE Atx7 and Htt sequester HSJ1a into aggregates. As is the critical role of HSJ1a in modulating cellular Atx3 proteostasis[45], we therefore inferred that the PQE proteins may disturb Atx3 proteostasis through interfering with the function of HSJ1. To address this issue, we investigated the effect of the PQE proteins on
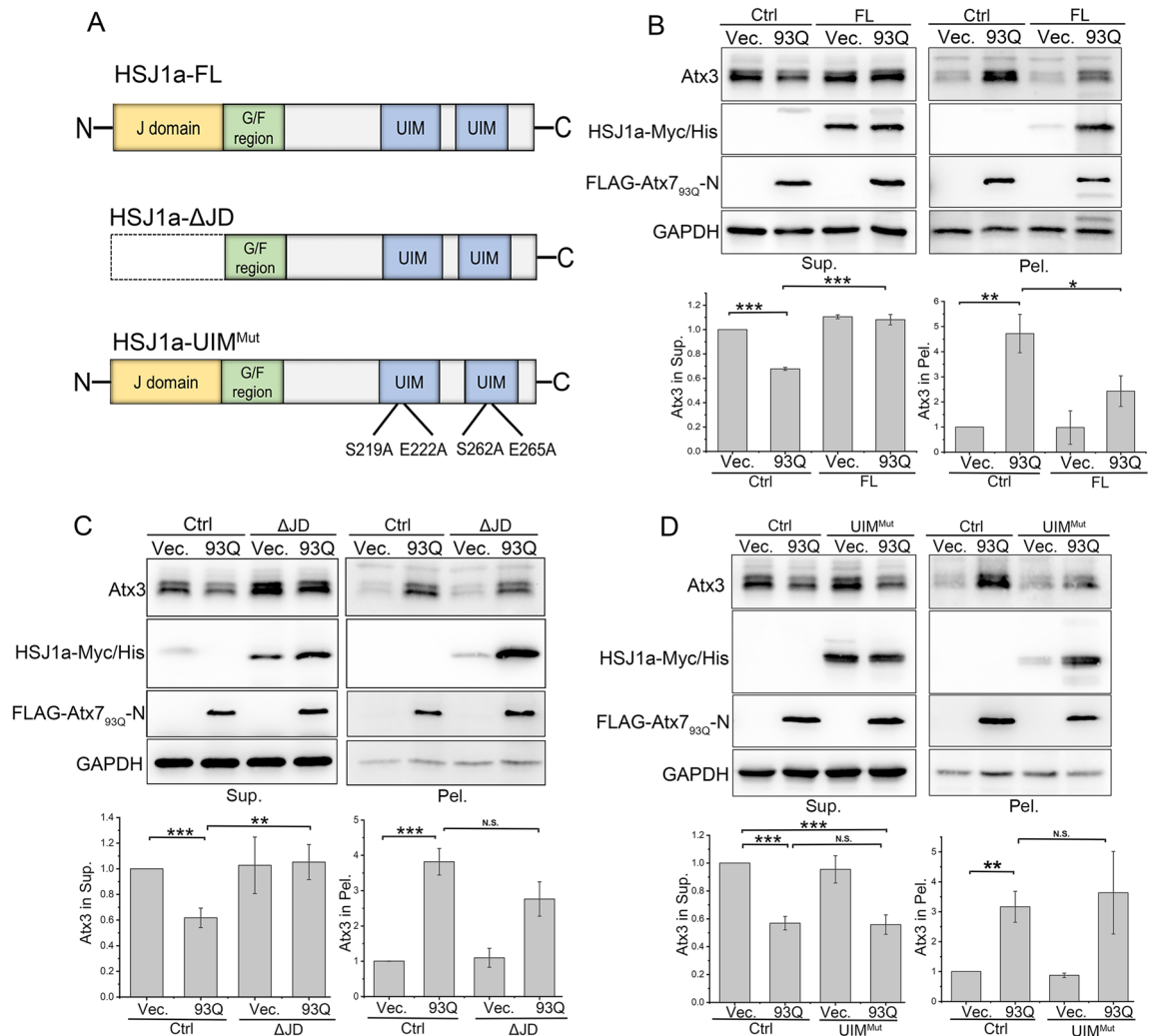
Figure 4. HSJ1a suppresses the degradation of Atx3 through its UIM domain. (**A**) Domain architectures of the HSJ1a protein and its mutants applied. (**B**) Overexpression of HSJ1a alleviates the decline of soluble Atx3 but still increases the aggregates caused by Atx7$_{93Q}$-N172. (**C**) As in (**B**), HSJ1a-ΔJD. (**D**) Overexpression of HSJ1a-UIM^{Mut} fails to suppress the decline of soluble Atx3 caused by Atx7$_{93Q}$-N172. HSJ1a-Myc/His or its mutants (HSJ1a-ΔJD and HSJ1a-UIM^{Mut}) was co-expressed with Atx7$_{93Q}$-N172 in HEK 293T cells. The pcDNA3.1-Myc/His plasmid was set as a control (Ctrl). The cell lysates were subjected to supernatant/pellet fractionation and Western blotting. Indicated proteins were detected by using anti-FLAG, anti-Myc, anti-Atx3 and anti-GAPDH antibodies. Sup., supernatant; Pel., pellet. Data are shown as Means ± SEM (n = 3). *$p < 0.05$; **$p < 0.01$; ***$p < 0.001$; N.S., no significance.

HSJ1 in cells. As shown (Supplemental Fig. 4), upon expression of Atx7$_{93Q}$-N172 or NLS-Atx7$_{93Q}$-N172, exogenous HSJ1a in the pellet fraction increased significantly, whereas it remained unchanged in the supernatant. We then examined the effects of these PQE Atx7 and Htt on the endogenous HSJ1, mainly HSJ1a and HSJ1b forms. The protein level of endogenous HSJ1 in pellet became much higher upon expression of Atx7$_{93Q}$-N172 (Fig. 5A), NLS-Atx7$_{93Q}$-N172 (Fig. 5B) or Htt$_{100Q}$-N90 (Fig. 5C), as compared with that of the control vector. There is a slight decrease of the HSJ1 level in supernatant when over-expressing the nucleus-localized form (Fig. 5B), which was not observed in the cytoplasmic forms. Thus, HSJ1 may be sequestered into the aggregates by the PQE proteins. For further confirmation, we observed the cellular localizations of HSJ1 and the polyQ inclusions by confocal microscopy. The images showed that endogenous HSJ1 was well co-localized with the inclusions formed by these three polyQ proteins (Fig. 5D, E). Together, these data demonstrate that the PQE proteins can sequester HSJ1 into their aggregates or inclusions.

Importance of the UIM domain of HSJ1 in sequestration by the PQE proteins. According to our hypothesis, molecular interactions are the prerequisite for sequestration by protein aggregates[40,54]. To better understand the mechanism underlying the sequestration effect of PQE proteins on HSJ1, we constructed two domain-deleted mutants of HSJ1a, HSJ1a-ΔJD and HSJ1a-ΔUIM, and visualized their co-localization with the nuclear polyQ inclusions. As shown, full-length HSJ1a was localized to the inclusions formed by NLS-Atx7$_{93Q}$-
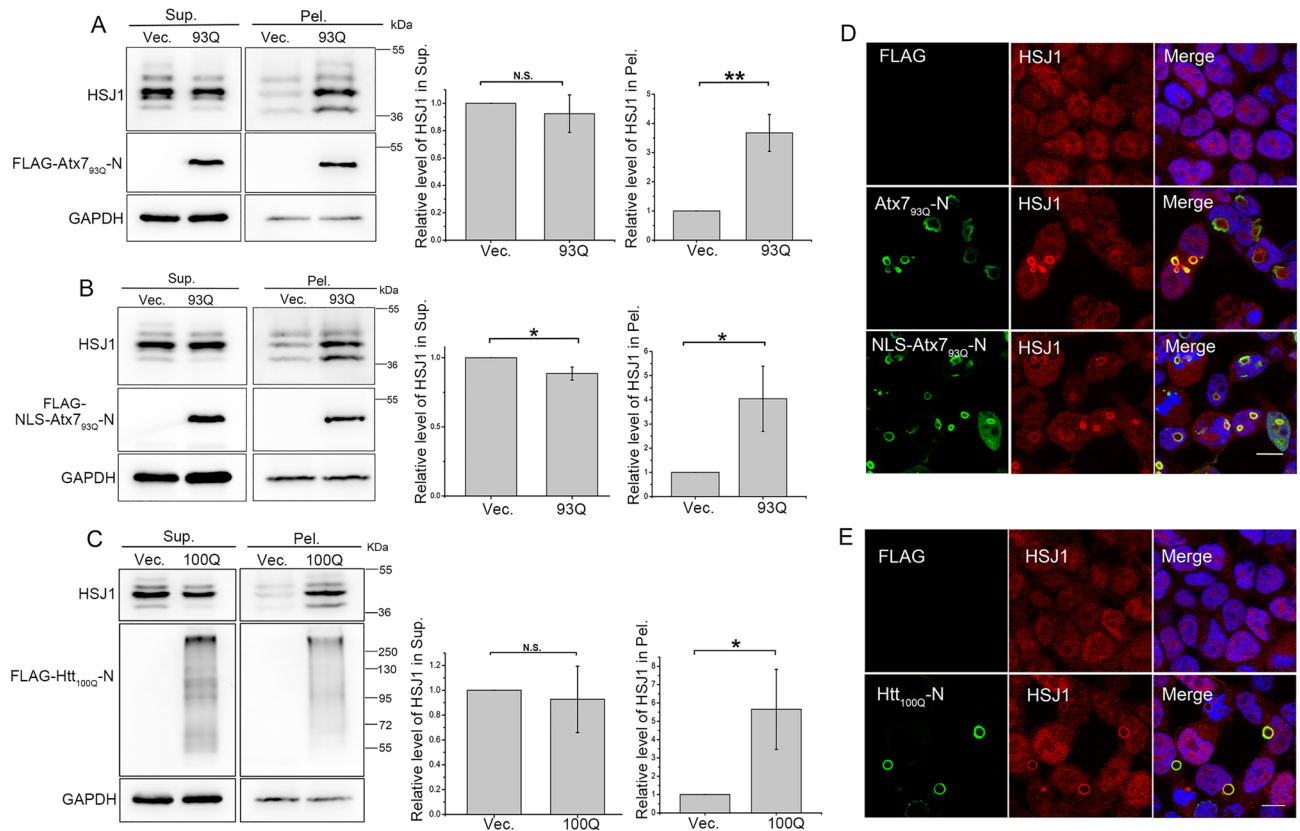
Figure 5. PQE Atx7 and Htt sequester endogenous HSJ1 into aggregates. (**A**) Sequestration of endogenous HSJ1 by $Atx7_{93Q}$-N172. (**B**) As in (**A**), by $NLS-Atx7_{93Q}$-N172. (**C**) As in (**A**), by Htt_{100Q}-N90. HEK 293T cells were transfected with each indicated plasmid and the lysates were subjected to supernatant/pellet fractionation and Western blotting. Indicated proteins were detected by using anti-FLAG, anti-HSJ1 and anti-GAPDH antibodies. The three main bands indicate different isoforms of endogenous HSJ1. Sup., supernatant; Pel., pellet. Data are shown as Means ± SEM (n = 3). *$p < 0.05$; **$p < 0.01$; N.S., no significance. (**D**) Immunofluorescence imaging showing that $Atx7_{93Q}$-N172 sequesters endogenous HSJ1 into inclusions. (**E**) As in (**D**), Htt_{100Q}-N90. HEK 293T cells were transfected with indicated plasmids and then subjected to immunofluorescence imaging. PolyQ proteins were stained with anti-FLAG antibody (green), HSJ1 was stained with anti-HSJ1 antibody (red), and nuclei were stained with Hoechst (blue). Scale bar = 10 μm.

N172 in nuclei, while the JD-deleted mutant was also observed well co-localized with the polyQ inclusions in nuclei, but deletion of UIM disrupted their co-localization in the inclusions (Supplemental Fig. 5). It suggests that the UIM domain of HSJ1a may be critical for its being sequestered into the polyQ aggregates or inclusions. We then applied the HSJ1a-UIM^{mut} mutant and examined the sequestration efficiency by the nucleus-localized form of $Atx7_{93Q}$-N172. The result showed that the sequestered protein level of the UIM mutant of HSJ1a was much lower than that of the WT (Fig. 6A). Consistently, as observed by confocal microscopy, the UIM mutation significantly alleviated the localization of HSJ1a into the polyQ inclusions formed by $NLS-Atx7_{93Q}$-N172 in nuclei (Fig. 6B). Thus, the UIM domain of HSJ1 is important to be sequestered into the polyQ aggregates or inclusions, which implies the specific interaction of HSJ1 with the Ub moieties conjugated in the polyQ proteins[55].

Discussion
The PQE protein aggregates disrupt cellular proteostasis of Atx3.
As the pathogenic protein of SCA3, PQE Atx3 has received quite a lot of attention from the researchers[43]. In the recent years, WT Atx3 has been found in the inclusion bodies or aggresomes formed by the misfolded CFTR mutant (CFTR-ΔF508)[41], SOD1[42] and even PQE Atx3 itself[17,44]. Thus, uncovering the link between Atx3 with those disease-related polyQ proteins is of great importance, but up to date, limited work has been done to elucidate this issue. As reported, WT Atx3 was passively sequestered into polyQ aggregates or inclusions by the co-aggregation of common polyQ sequences[17,44], which may contribute to the reducing effect of the soluble or functionally available fraction of Atx3 in cell. We have revealed for the first time that the PQE proteins disrupt the protein balance of intracellular Atx3 through sequestering the co-chaperone HSJ1 into aggregates or inclusions. Specially, the PQE proteins promote the proteasomal degradation of endogenous Atx3 massively, leading to a remarkable reduction of the soluble Atx3 (Fig. 1). Besides, they can also enhance formation of the Atx3 aggregates accumulated in the inclusions. This accumulation of Atx3 aggregates, from our point of view, may be partially due to the increased misfolding and aggregation of Atx3 or attributed to the co-aggregation effect between the common and the expanded
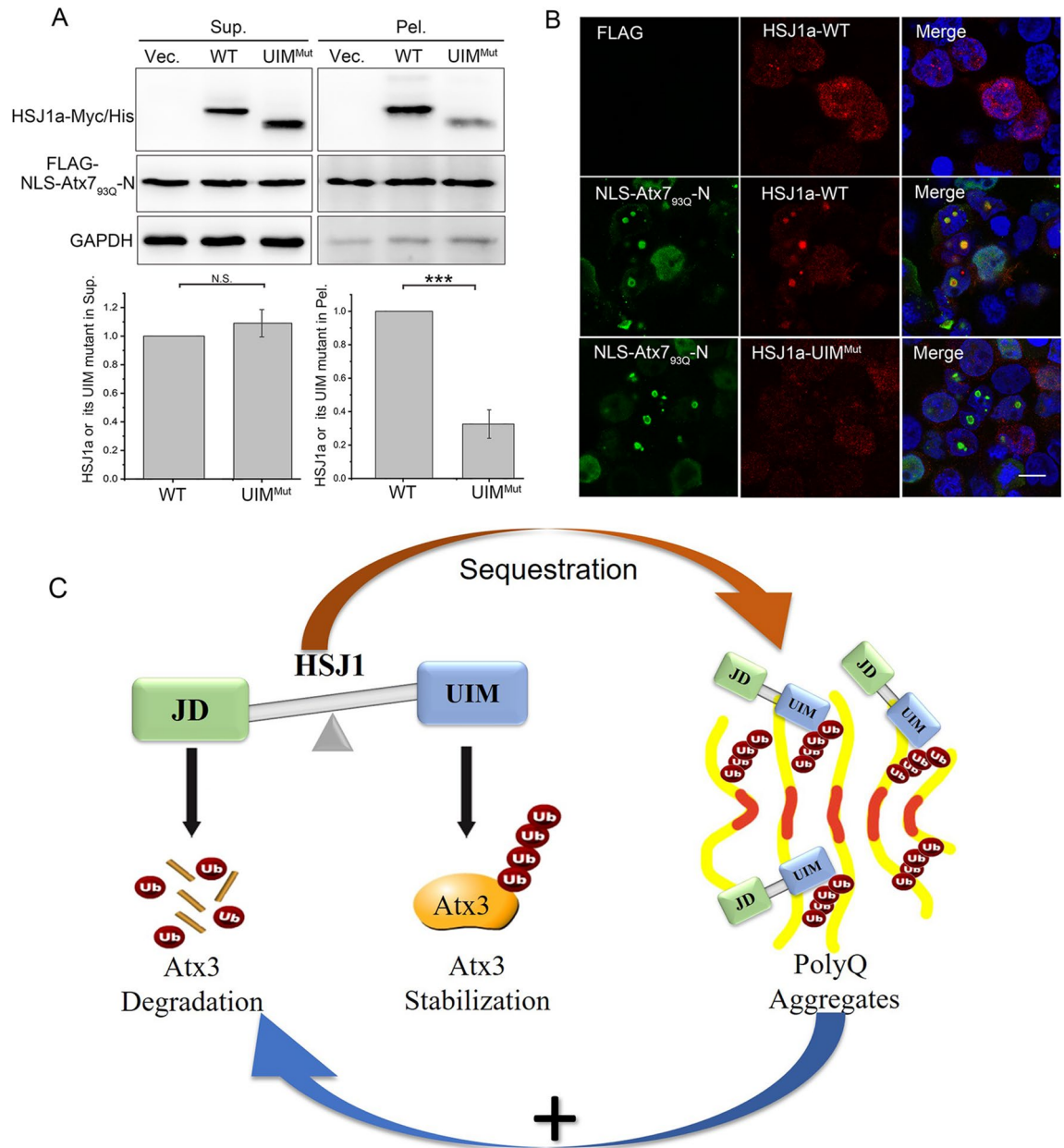
Figure 6. Sequestration of HSJ1 by the polyQ aggregates is mediated by the UIM domain of HSJ1. (**A**) UIM mutation suppresses the sequestration of HSJ1a into aggregates. HSJ1a-Myc/His or its UIM mutant was co-expressed with NLS-Atx7$_{93Q}$-N172 in HEK 293T cells, the cell lysates were subjected to supernatant/pellet fractionation, then HSJ1a or its UIM mutant was detected by Western blotting. Sup., supernatant; Pel., pellet. Data are shown as Means ± SEM (n = 3). ***$p < 0.001$. N.S., no significance. (**B**) Sequestration of HSJ1a or its UIM mutant into polyQ inclusions as visualized by confocal microscopy. HSJ1a-Myc/His or its UIM mutant was co-expressed with NLS-Atx7$_{93Q}$-N172 in HEK 293T cells, then the cells were subjected to immunofluorescence imaging. NLS-Atx7$_{93Q}$-N172 were stained with anti-FLAG antibody (green), HSJ1a-Myc/His or its UIM mutant was stained with anti-Myc/His antibody (red), and nuclei were stained with Hoechst (blue). Scale bar = 10 μm. (**C**) Schematic representation of the impaired proteostasis of Atx3 caused by polyQ aggregates through sequestration of HSJ1. Under the normal conditions, HSJ1 balances the degradation and stabilization of Atx3 (brown) through coordinating the functions of its JD and UIM domains, and thus maintains the cellular proteostasis of Atx3. The PQE protein (yellow) forms insoluble aggregates via its polyQ tract (red bar), interacts with HSJ1 via its conjugated Ub molecules (red ball), and sequesters HSJ1 into the aggregates. The sequestration of HSJ1 may cause depletion or dysfunction of the co-chaperone and consequently impairs the cellular proteostasis of Atx3.

polyQ sequences. The severe damage of the proteostasis of intracellular Atx3 may further influence its normal function. Similar case has also been reported that the normal function of Atx3 in stabilization of CREB-binding

protein (CBP) may be destroyed by mutant Htt, and consequently lead to dysregulation of the CBP-related gene expression[56]. It is likely that the loss-of-function effect of Atx3 resulted from disruption of the cellular proteostasis may account for one of the pathologies in Huntington's disease.

HSJ1 functions in modulating the cellular proteostasis of Atx3. The HSJ1 protein is an essential player orchestrating the proteostasis in nerve cells[46,57], for example, overexpression of HSJ1a is probable to reduce aggregation of mutant (PQE) Htt and enhance its solubility[58]. Mutations in HSJ1 are found to be closely related to the pathologies of diverse neurodegenerative disorders[59–61]. Work in our laboratory has identified HSJ1 as a regulator of both the WT and pathogenic Atx3 protein[45], which further emphasizes the importance of HSJ1 in cellular proteostasis and proteinopathy. HSJ1 exhibits dual roles in regulating the degradation and stabilization of Atx3 through its JD and UIM domains, respectively. The JD and UIM domains of HSJ1 seem to delicately maintain the balance of the cellular Atx3 protein in a *Yin-Yang* manner. However, expression of the PQE proteins significantly destroys this internal balance, leading to the massive degradation of soluble Atx3. Overexpression of the full-length or JD-deleted HSJ1a rather than the UIM-mutated one can efficiently suppress the degradation of Atx3 and reverse its protein level, which confirms the role of the UIM domain of HSJ1 in maintaining the Atx3 stability[45]. Apart from the function in modulating protein stability, HSJ1 also exhibits a chaperoning activity by binding with HSP70 and promoting proteasomal degradation, which to some extent attenuates formation of the Atx3 aggregates. The anti-aggregation role of the HSP40 co-chaperones has also been documented in other literatures[62–64], making it a potential candidate of drug targets for manipulating the amyloid related diseases.

Sequestration of HSJ1 by the polyQ aggregates. Accumulating evidence has shown that molecular chaperones are the common components accumulated in inclusion bodies[7,35]. As a member of the co-chaperone family, HSJ1 has also been observed in polyQ inclusions[36,45]. This study corroborates the previous finding that HSJ1 can be accumulated in the aggregates or inclusions through interacting with the PQE proteins (Fig. 5). According to our hijacking hypothesis raised previously[40], HSJ1 could be sequestered into the polyQ aggregates or inclusions that may cause dysfunction of the co-chaperone. We propose that this sequestration effect partially contributes to the proteinopathies of polyQ proteins. Since the chaperone and co-chaperone components play a central effect in protein quality control (PQC), the excessive occupation or sequestration of those proteins may thus destroy the integrity and homeostasis of the intracellular proteome. For example, sequestration of Sis1p (an HSP40-like co-chaperone in yeast) into the polyQ aggregates results in inefficient degradation of the cytoplasmic misfolded proteins and disruption of their cellular proteostasis[39]. Our results demonstrate that HSJ1 could be sequestered into the polyQ aggregates through its UIM domain (Fig. 6A, B). Analogous to our previous finding that the PQE proteins sequester Ub adaptors into aggregates via conjugated Ub chains[24], we speculate that the PQE protein fragments (Atx7$_{93Q}$-N172 and Htt$_{100Q}$-N90) that are prone to forming aggregates are highly ubiquitinated[55], so that they are capable of binding with HSJ1 on its UIM domain. Considering the function of HSJ1 in maintaining the balance of cellular Atx3, the PQE proteins impair the cellular proteostasis of Atx3 by sequestering HSJ1 into aggregates and causing the functional depletion or dysfunction of HSJ1 through UIM-Ub interactions.

The PQE proteins disturb the modulating balance of HSJ1 on endogenous Atx3 by the sequestration effect. Our laboratory has proposed that protein aggregates sequester essential cellular components and thus cause the loss-of-function effect[40], which may explain why protein aggregates are toxic to cells. Considering the importance of HSJ1 in maintaining the balance of cellular Atx3, we conclude that the PQE proteins impair cellular proteostasis of Atx3 through sequestering HSJ1 into aggregates and consequently causing functional loss of HSJ1 (Fig. 6C). Specifically, under normal conditions, the cellular proteostasis of Atx3 is sophisticatedly balanced by the co-chaperone HSJ1, in which the J domain mediates proteasomal degradation of Atx3 while the UIM domain stabilizes the ubiquitinated Atx3[45]. However, the PQE protein may experience ubiquitination that confers it to interact with the UIM domain of HSJ1; as a result, the cellular HSJ1 protein will be massively sequestered into the ubiquitinated polyQ aggregates. In this way, HSJ1 may be depleted by both sequestration into the insoluble polyQ aggregates and aberrant interactions with the Ub-conjugated protein monomers or oligomers. Depletion of the co-chaperone from its functionally available fraction will consequently break down the balance between degradation and stabilization of the Atx3 protein (Fig. 6C). Besides, this study also provides additional evidence in supporting the hijacking model that sequestration of cellular essential components by protein aggregates may account for the pathologies of aggregation-related neurodegenerative diseases.

Materials and methods

Plasmids, antibodies, and reagents. The cDNAs for encoding Atx7$_{93Q}$-N172 (residues 1–172) and Htt$_{100Q}$-N90 (residues 1–90) were cloned into the FLAG-pcDNA3.1 vector as stored in our laboratory[45]. To construct a nucleus-localized expression plasmid, the DNA sequence for nuclear localization signal (NLS, PKKKRKV) was introduced right before that of Atx7$_{93Q}$-N172. The cDNAs for encoding full-length HSJ1a (residues 1–274), HSJ1a-ΔJD (residues 91–274), HSJ1a-ΔUIM (residues 1–207) and HSJ1a-UIM^{Mut} (S219A/E222A/S262A/E265A) were cloned into the Myc/His-pcDNA3.0 vector[45] (Supplemental Table 1). The antibody against FLAG was purchased from Sigma and anti-Atx3 was from Abclonal. The anti-HSJ1, anti-β-actin and anti-GAPDH antibodies were from Proteintech; anti-Myc and anti-LC3B were purchased from Cell Signaling (Supplemental Table 2). All secondary antibodies were from Jackson ImmunoResearch Laboratories. MG132 was purchased from Cell Signaling and chloroquine (CQ) diphosphate was from Sigma.

Cell culture and transfection. As described previously[25], cells were cultured in DMEM (HyClone) supplemented with 10% fetal bovine serum (Gemini) and penicillin–streptomycin at 37 °C under a humidified atmosphere containing 5% CO_2. Transfections of all the plasmids into HEK 293T cells were performed by using *PolyJet* reagent (SignaGen) following the manufacturer's instructions.

Supernatant/pellet fractionation. HEK 293T cells were harvested about 48 h after transfection and lysed in 100 μL of a RIPA buffer (50 mM Tris–HCl, pH 7.5, 150 mM NaCl, 1 mM EDTA, 1% Nonidet P-40, and protease inhibitor mixture) on ice for 30 min, and then centrifuged at 16,200*g* for 15 min at 4 °C. The supernatant was added with 100 μL of 2× loading buffer (2% SDS), while the pellet was sufficiently washed with the RIPA buffer for three times at 4 °C before added with 40 μL of 4× loading buffer (4% SDS)[24]. Samples acquired through the above process were then subjected to SDS-PAGE and Western blotting.

Extraction of total Atx3 protein. The cultured cells were harvested about 48 h after transfection, and lysed with 100 μL of the RIPA buffer containing 8 M urea on ice for 30 min for dissolving all aggregated forms of Atx3. The lysates were then added with 100 μL of 2× loading buffer (2% SDS) that also contains 8 M urea. The protein samples acquired through the above method were then boiled to denature and subjected to SDS-PAGE and Western blotting.

Western blotting analysis. The protein samples of lysates or fractions were subjected to SDS-PAGE and transferred onto PVDF membranes (PerkinElmer). When needed, the blots had been cut prior to antibody hybridization. The indicated proteins were detected with specific primary and secondary antibodies and visualized by using an ECL detection kit (Thermo Scientific) as previously described[65]. For quantification, the integral grayscale values of protein bands were recorded by using *Scion Image* or *ImageJ* software. All the original unprocessed gel images are provided in the Supplementary Information file.

Immunofluorescence microscopy. The method for preparing samples for confocal imaging was similar to that described previously[24]. HEK 293T cells grown on glass coverslips were transfected with indicated plasmids by *PolyJet* reagent. About 48 h after transfection, the cells were fixed with 4% paraformaldehyde for 15 min, permeabilized with 0.1% Triton X-100 and then blocked with the blocking solution (5% BSA and 10% FBS in a PBS buffer) for 1 h. All the above processes were performed at room temperature. Then the cells were incubated with the respective primary antibodies against FLAG (1:100) and Atx3 (1:100), HSJ1 (1:100) or Myc (1:100) overnight at 4 °C. After washing with the PBS buffer for three times, the cells were labeled with FITC-conjugated anti-mouse antibody and TRITC-conjugated anti-rabbit antibody (1:100, Jackson ImmunoResearch Laboratories) for 1 h. The nuclei were stained with Hoechst (Sigma). All images were obtained on a Leica Microsystems TCS SP8 confocal microscope.

Quantitative RT-PCR assay. Total RNAs from cultured HEK 293T cells were extracted with TRIzol (Life Technologies) according to the manufacturer's protocol. The cDNAs were reversely transcribed with 4× Reverse Transcription Master Mix (EZBioscience) using 2-μg total RNA from each sample. Quantitative real-time PCR (qPCR) was performed using Hieff qPCR SYBR Green Master Mix (Yeasen Biotech) and analyzed on a LightCycler96 PCR system (Roche). The qPCR assay was carried out in a 20-μL reaction mixture (10 μL of SYBR, 2 μL of cDNA template and 0.5 mM each primer). GAPDH was chosen as the endogenous control for qPCR analysis. Three independent experiments were performed in this qPCR assay.

Statistical analysis. The data from at least three independent experiments were obtained from the gray values of specific protein bands in Western blots and normalized to that of the respective vector control. Then the relative levels for protein amounts were presented as Means ± SEM. Statistical analyses were performed with one-way ANOVA program by using *OriginPro* software. Differences were considered statistically significant at $p < 0.05$. In all experiments, the p values were labeled in the graphs with * ($p < 0.05$), ** ($p < 0.01$), *** ($p < 0.001$) and N.S. (no significance).

References

1. Adegbuyiro, A., Sedighi, F., Pilkington, A. W. T., Groover, S. & Legleiter, J. Proteins containing expanded polyglutamine tracts and neurodegenerative disease. *Biochemistry* **56**, 1199–1217. https://doi.org/10.1021/acs.biochem.6b00936 (2017).
2. Lieberman, A. P., Shakkottai, V. G. & Albin, R. L. Polyglutamine repeats in neurodegenerative diseases. *Annu. Rev. Pathol.* **14**, 1–27. https://doi.org/10.1146/annurev-pathmechdis-012418-012857 (2019).
3. Saunders, H. M. & Bottomley, S. P. Multi-domain misfolding: Understanding the aggregation pathway of polyglutamine proteins. *Protein Eng. Des. Sel.* **22**, 447–451. https://doi.org/10.1093/protein/gzp033 (2009).
4. Gabr, M. T. & Peccati, F. Dual targeting of monomeric tau and alpha-synuclein aggregation: A new multitarget therapeutic strategy for neurodegeneration. *ACS Chem. Neurosci.* **11**, 2051–2057. https://doi.org/10.1021/acschemneuro.0c00281 (2020).
5. Liscic, R. M. & Breljak, D. Molecular basis of amyotrophic lateral sclerosis. *Prog. Neuropsychopharmacol. Biol. Psychiatry* **35**, 370–372. https://doi.org/10.1016/j.pnpbp.2010.07.017 (2011).
6. Jimenez-Sanchez, M., Licitra, F., Underwood, B. R. & Rubinsztein, D. C. Huntington's disease: Mechanisms of pathogenesis and therapeutic strategies. *Cold Spring Harb Perspect Med* https://doi.org/10.1101/cshperspect.a024240 (2017).

7. Niewiadomska-Cimicka, A. & Trottier, Y. Molecular targets and therapeutic strategies in spinocerebellar ataxia type 7. *Neurotherapeutics* **16**, 1074–1096. https://doi.org/10.1007/s13311-019-00778-5 (2019).

8. McLoughlin, H. S., Moore, L. R. & Paulson, H. L. Pathogenesis of SCA3 and implications for other polyglutamine diseases. *Neurobiol. Dis.* **134**, 104635. https://doi.org/10.1016/j.nbd.2019.104635 (2020).

9. Pearce, M. M. P. & Kopito, R. R. Prion-like characteristics of polyglutamine-containing proteins. *Cold Spring Harb. Perspect. Med.* https://doi.org/10.1101/cshperspect.a024257 (2018).

10. Matos, C. A., Almeida, L. P. & Nobrega, C. Proteolytic cleavage of polyglutamine disease-causing proteins: Revisiting the toxic fragment hypothesis. *Curr. Pharm. Des.* **23**, 753–775. https://doi.org/10.2174/1381612822666161227121912 (2017).

11. Graham, R. K. *et al.* Cleavage at the caspase-6 site is required for neuronal dysfunction and degeneration due to mutant huntingtin. *Cell* **125**, 1179–1191. https://doi.org/10.1016/j.cell.2006.04.026 (2006).

12. Graham, R. K. *et al.* Cleavage at the 586 amino acid caspase-6 site in mutant huntingtin influences caspase-6 activation in vivo. *J. Neurosci.* **30**, 15019–15029. https://doi.org/10.1523/JNEUROSCI.2071-10.2010 (2010).

13. Landles, C. *et al.* Proteolysis of mutant huntingtin produces an exon 1 fragment that accumulates as an aggregated protein in neuronal nuclei in Huntington disease. *J. Biol. Chem.* **285**, 8808–8823. https://doi.org/10.1074/jbc.M109.075028 (2010).

14. Garden, G. A. *et al.* Polyglutamine-expanded ataxin-7 promotes non-cell-autonomous purkinje cell degeneration and displays proteolytic cleavage in ataxic transgenic mice. *J. Neurosci.* **22**, 4897–4905 (2002).

15. Guyenet, S. J. *et al.* Proteolytic cleavage of ataxin-7 promotes SCA7 retinal degeneration and neurological dysfunction. *Hum. Mol. Genet.* **24**, 3908–3917. https://doi.org/10.1093/hmg/ddv121 (2015).

16. Young, J. E. *et al.* Proteolytic cleavage of ataxin-7 by caspase-7 modulates cellular toxicity and transcriptional dysregulation. *J. Biol. Chem.* **282**, 30150–30160. https://doi.org/10.1074/jbc.M705265200 (2007).

17. Haacke, A. *et al.* Proteolytic cleavage of polyglutamine-expanded ataxin-3 is critical for aggregation and sequestration of non-expanded ataxin-3. *Hum Mol Genet* **15**, 555–568. https://doi.org/10.1093/hmg/ddi472 (2006).

18. Haacke, A., Hartl, F. U. & Breuer, P. Calpain inhibition is sufficient to suppress aggregation of polyglutamine-expanded ataxin-3. *J. Biol. Chem.* **282**, 18851–18856. https://doi.org/10.1074/jbc.M611914200 (2007).

19. Hubener, J. *et al.* Calpain-mediated ataxin-3 cleavage in the molecular pathogenesis of spinocerebellar ataxia type 3 (SCA3). *Hum. Mol. Genet.* **22**, 508–518. https://doi.org/10.1093/hmg/dds449 (2013).

20. Simoes, A. T. *et al.* Calpastatin-mediated inhibition of calpains in the mouse brain prevents mutant ataxin 3 proteolysis, nuclear localization and aggregation, relieving Machado-Joseph disease. *Brain J. Neurol.* **135**, 2428–2439. https://doi.org/10.1093/brain/aws177 (2012).

21. Ratovitski, T. *et al.* Mutant huntingtin N-terminal fragments of specific size mediate aggregation and toxicity in neuronal cells. *J. Biol. Chem.* **284**, 10855–10867. https://doi.org/10.1074/jbc.M804813200 (2009).

22. Schilling, G. *et al.* Intranuclear inclusions and neuritic aggregates in transgenic mice expressing a mutant N-terminal fragment of huntingtin. *Hum Mol Genet* **8**, 397–407. https://doi.org/10.1093/hmg/8.3.397 (1999).

23. Jiang, Y. J. *et al.* Interaction with polyglutamine-expanded huntingtin alters cellular distribution and RNA processing of huntingtin yeast two-hybrid protein A (HYPA). *J. Biol. Chem.* **286**, 25236–25245. https://doi.org/10.1074/jbc.M110.216333 (2011).

24. Yang, H. *et al.* PolyQ-expanded huntingtin and ataxin-3 sequester ubiquitin adaptors hHR23B and UBQLN2 into aggregates via conjugated ubiquitin. *FASEB J.* **32**, 2923–2933. https://doi.org/10.1096/fj.201700801RR (2018).

25. Yang, H. *et al.* Aggregation of polyglutamine-expanded ataxin-3 sequesters its specific interacting partners into inclusions: Implication in a loss-of-function pathology. *Sci. Rep.* **4**, 6410. https://doi.org/10.1038/srep06410 (2014).

26. Yang, H. *et al.* Aggregation of polyglutamine-expanded ataxin 7 protein specifically sequesters ubiquitin-specific protease 22 and deteriorates its deubiquitinating function in the Spt-Ada-Gcn5-acetyltransferase (SAGA) complex. *J. Biol. Chem.* **290**, 21996–22004. https://doi.org/10.1074/jbc.M114.631663 (2015).

27. Hartl, F. U. Protein misfolding diseases. *Annu. Rev. Biochem.* **86**, 21–26. https://doi.org/10.1146/annurev-biochem-061516-044518 (2017).

28. Kim, Y. E. *et al.* Soluble oligomers of PolyQ-expanded Huntingtin target a multiplicity of key cellular factors. *Mol. Cell* **63**, 951–964. https://doi.org/10.1016/j.molcel.2016.07.022 (2016).

29. Benilova, I., Karran, E. & De Strooper, B. The toxic Abeta oligomer and Alzheimer's disease: An emperor in need of clothes. *Nat. Neurosci.* **15**, 349–357. https://doi.org/10.1038/nn.3028 (2012).

30. Roberts, H. L. & Brown, D. R. Seeking a mechanism for the toxicity of oligomeric alpha-synuclein. *Biomolecules* **5**, 282–305. https://doi.org/10.3390/biom5020282 (2015).

31. Bauerlein, F. J. B. *et al.* In situ architecture and cellular interactions of PolyQ inclusions. *Cell* **171**, 179–187. https://doi.org/10.1016/j.cell.2017.08.009 (2017).

32. Johnston, J. A., Dalton, M. J., Gurney, M. E. & Kopito, R. R. Formation of high molecular weight complexes of mutant Cu, Zn-superoxide dismutase in a mouse model for familial amyotrophic lateral sclerosis. *Proc. Natl. Acad. Sci. U.S.A.* **97**, 12571–12576. https://doi.org/10.1073/pnas.220417997 (2000).

33. Latouche, M. *et al.* Polyglutamine and polyalanine expansions in ataxin7 result in different types of aggregation and levels of toxicity. *Mol. Cell Neurosci.* **31**, 438–445. https://doi.org/10.1016/j.mcn.2005.10.013 (2006).

34. Cummings, C. J. *et al.* Chaperone suppression of aggregation and altered subcellular proteasome localization imply protein misfolding in SCA1. *Nat. Genet.* **19**, 148–154. https://doi.org/10.1038/502 (1998).

35. Jana, N. R., Tanaka, M., Wang, G. & Nukina, N. Polyglutamine length-dependent interaction of Hsp40 and Hsp70 family chaperones with truncated N-terminal huntingtin: Their role in suppression of aggregation and cellular toxicity. *Hum. Mol. Genet.* **9**, 2009–2018. https://doi.org/10.1093/hmg/9.13.2009 (2000).

36. Shirasaki, D. I. *et al.* Network organization of the huntingtin proteomic interactome in mammalian brain. *Neuron* **75**, 41–57. https://doi.org/10.1016/j.neuron.2012.05.024 (2012).

37. Chai, Y., Koppenhafer, S. L., Shoesmith, S. J., Perez, M. K. & Paulson, H. L. Evidence for proteasome involvement in polyglutamine disease: Localization to nuclear inclusions in SCA3/MJD and suppression of polyglutamine aggregation in vitro. *Hum. Mol. Genet.* **8**, 673–682. https://doi.org/10.1093/hmg/8.4.673 (1999).

38. Lowe, J. *et al.* Ubiquitin is a common factor in intermediate filament inclusion bodies of diverse type in man, including those of Parkinson's disease, Pick's disease, and Alzheimer's disease, as well as Rosenthal fibres in cerebellar astrocytomas, cytoplasmic bodies in muscle, and mallory bodies in alcoholic liver disease. *J. Pathol.* **155**, 9–15. https://doi.org/10.1002/path.1711550105 (1988).

39. Park, S. H. *et al.* PolyQ proteins interfere with nuclear degradation of cytosolic proteins by sequestering the Sis1p chaperone. *Cell* **154**, 134–145. https://doi.org/10.1016/j.cell.2013.06.003 (2013).

40. Yang, H. & Hu, H. Y. Sequestration of cellular interacting partners by protein aggregates: Implication in a loss-of-function pathology. *FEBS J* **283**, 3705–3717. https://doi.org/10.1111/febs.13722 (2016).

41. Burnett, B. G. & Pittman, R. N. The polyglutamine neurodegenerative protein ataxin 3 regulates aggresome formation. *Proc. Natl. Acad. Sci. U.S.A.* **102**, 4330–4335. https://doi.org/10.1073/pnas.0407252102 (2005).

42. Wang, H., Ying, Z. & Wang, G. Ataxin-3 regulates aggresome formation of copper-zinc superoxide dismutase (SOD1) by editing K63-linked polyubiquitin chains. *J. Biol. Chem.* **287**, 28576–28585. https://doi.org/10.1074/jbc.M111.299990 (2012).

43. Da Silva, J. D., Teixeira-Castro, A. & Maciel, P. From pathogenesis to novel therapeutics for spinocerebellar Ataxia Type 3: Evading potholes on the way to translation. *Neurotherapeutics* **16**, 1009–1031. https://doi.org/10.1007/s13311-019-00798-1 (2019).

44. Jia, N. L., Fei, E. K., Ying, Z., Wang, H. F. & Wang, G. H. PolyQ-expanded ataxin-3 interacts with full-length ataxin-3 in a polyQ length-dependent manner. *Neurosci. Bull.* **24**, 201–208. https://doi.org/10.1007/s12264-008-0326-9 (2008).
45. Gao, X. C. *et al.* Co-chaperone HSJ1a dually regulates the proteasomal degradation of ataxin-3. *PLoS ONE* **6**, e19763. https://doi.org/10.1371/journal.pone.0019763 (2011).
46. Zarouchlioti, C., Parfitt, D. A., Li, W., Gittings, L. M. & Cheetham, M. E. DNAJ Proteins in neurodegeneration: Essential and protective factors. *Philos. Trans. R Soc. Lond. B Biol. Sci.* https://doi.org/10.1098/rstb.2016.0534 (2018).
47. Duncan, E. J., Cheetham, M. E., Chapple, J. P. & van der Spuy, J. The role of HSP70 and its co-chaperones in protein misfolding, aggregation and disease. *Subcell. Biochem.* **78**, 243–273. https://doi.org/10.1007/978-3-319-11731-7_12 (2015).
48. Balchin, D., Hayer-Hartl, M. & Hartl, F. U. In vivo aspects of protein folding and quality control. *Science* https://doi.org/10.1126/science.aac4354 (2016).
49. Hipp, M. S., Park, S. H. & Hartl, F. U. Proteostasis impairment in protein-misfolding and -aggregation diseases. *Trends Cell Biol.* **24**, 506–514. https://doi.org/10.1016/j.tcb.2014.05.003 (2014).
50. Kim, Y. E., Hipp, M. S., Bracher, A., Hayer-Hartl, M. & Hartl, F. U. Molecular chaperone functions in protein folding and proteostasis. *Annu. Rev. Biochem.* **82**, 323–355. https://doi.org/10.1146/annurev-biochem-060208-092442 (2013).
51. Gao, X. & Hu, H. Quality control of the proteins associated with neurodegenerative diseases. *Acta Biochim. Biophys. Sin. (Shanghai)* **40**, 612–618 (2008).
52. Cheng, C. & Liu, Z. G. Autophagy and the metabolism of misfolding protein. *Adv. Exp. Med. Biol.* **1206**, 375–420. https://doi.org/10.1007/978-981-15-0602-4_18 (2019).
53. Ciechanover, A. & Kwon, Y. T. Degradation of misfolded proteins in neurodegenerative diseases: Therapeutic targets and strategies. *Exp. Mol. Med.* **47**, e147. https://doi.org/10.1038/emm.2014.117 (2015).
54. Yue, H. W. & Hu, H. Y. Sequestration of cellular essential proteins or RNA by polyglutamine-expanded protein aggregates. *Prog. Biochem. Biophys.* **45**, 1204–1213. https://doi.org/10.16476/j.pibb.2018.0141 (2018).
55. Hakim-Eshed, V. *et al.* Site-specific ubiquitination of pathogenic huntingtin attenuates its deleterious effects. *Proc. Natl. Acad. Sci. U.S.A.* **117**, 18661–18669. https://doi.org/10.1073/pnas.2007667117 (2020).
56. Gao, R. *et al.* Mutant huntingtin impairs PNKP and ATXN3, disrupting DNA repair and transcription. *eLife* https://doi.org/10.7554/eLife.42988 (2019).
57. Qiu, X. B., Shao, Y. M., Miao, S. & Wang, L. The diversity of the DnaJ/Hsp40 family, the crucial partners for Hsp70 chaperones. *Cell Mol. Life Sci.* **63**, 2560–2570. https://doi.org/10.1007/s00018-006-6192-6 (2006).
58. Labbadia, J. *et al.* Suppression of protein aggregation by chaperone modification of high molecular weight complexes. *Brain J. Neurol.* **135**, 1180–1196. https://doi.org/10.1093/brain/aws022 (2012).
59. Blumen, S. C. *et al.* A rare recessive distal hereditary motor neuropathy with HSJ1 chaperone mutation. *Ann. Neurol.* **71**, 509–519. https://doi.org/10.1002/ana.22684 (2012).
60. Gess, B. *et al.* HSJ1-related hereditary neuropathies: Novel mutations and extended clinical spectrum. *Neurology* **83**, 1726–1732. https://doi.org/10.1212/WNL.0000000000000966 (2014).
61. Koutras, C. & Braun, J. E. J protein mutations and resulting proteostasis collapse. *Front. Cell. Neurosci.* **8**, 191. https://doi.org/10.3389/fncel.2014.00191 (2014).
62. Chen, H. J. *et al.* The heat shock response plays an important role in TDP-43 clearance: Evidence for dysfunction in amyotrophic lateral sclerosis. *Brain J. Neurol.* **139**, 1417–1432. https://doi.org/10.1093/brain/aww028 (2016).
63. Howarth, J. L. *et al.* Hsp40 molecules that target to the ubiquitin-proteasome system decrease inclusion formation in models of polyglutamine disease. *Mol. Ther.* **15**, 1100–1105. https://doi.org/10.1038/sj.mt.6300163 (2007).
64. Rose, J. M., Novoselov, S. S., Robinson, P. A. & Cheetham, M. E. Molecular chaperone-mediated rescue of mitophagy by a Parkin RING1 domain mutant. *Hum. Mol. Genet.* **20**, 16–27. https://doi.org/10.1093/hmg/ddq428 (2011).
65. He, W. T. *et al.* Cytoplasmic ubiquitin-specific protease 19 (USP19) modulates aggregation of polyglutamine-expanded Ataxin-3 and Huntingtin through the HSP90 Chaperone. *PLoS ONE* **11**, e0147515. https://doi.org/10.1371/journal.pone.0147515 (2016).

Acknowledgements

Author contributions

H.-W. Yue designed research, performed experiments, analyzed data, and wrote the original draft; J.-Y. Hong analyzed data and drew graphs; S.-X. Zhang analyzed data and drew graphs; L.-L. Jiang contributed cell culture and qPCR assay. H.-Y. Hu conceived and supervised the project and edited the manuscript.

Competing interests

The authors declare no competing interests.

Additional information

Supplementary Information The online version contains supplementary material available at https://doi.org/10.1038/s41598-021-87382-w.

Correspondence and requests for materials should be addressed to H.-Y.H.

Reprints and permissions information is available at www.nature.com/reprints.

Publisher's note Springer Nature remains neutral with regard to jurisdictional claims in published maps and institutional affiliations.